Asian Pub. Corp.

www.asianpubs.org

ARTICLE

Human Cancer Cells, Tissues and Tumors Treatment Using Dysprosium Nanoparticles

Alireza Heidari[1,2,✉], Katrina Schmitt[1], Maria Henderson[1] and Elizabeth Besana[1]

Asian Journal of Materials Chemistry

Volume: 4 Year: 2019
Issue: 3–4 Month: July–December
pp: 47–51
DOI: https://doi.org/10.14233/ajmc.2019.AJMC-P78

Received: 25 October 2019
Accepted: 7 December 2019
Published: 26 December 2019

ABSTRACT

In present study, thermoplasmonic characteristics of dysprosium nanoparticles with spherical, core-shell and rod shapes are investigated. In order to investigate these characteristics, interaction of synchrotron radiation emission as a function of the beam energy and dysprosium nanoparticles were simulated using 3D finite element method. Firstly, absorption and extinction cross-sections were calculated. Then, increases in temperature due to synchrotron radiation emission as a function of the beam energy absorption were calculated in dysprosium nanoparticles by solving heat equation. The results show that the dysprosium nanorods are more appropriate option for using in optothermal human cancer cells, tissues and tumors treatment method.

KEYWORDS

Dysprosium nanoparticles, 3D Finite element method, Optothermal, Thermoplasmonic, Synchrotron radiation, Beam energy.

INTRODUCTION

In recent decade, metallic nanoparticles have been widely interested due to their interesting optical characteristics [1-8]. Resonances of surface plasmon in these nanoparticles lead to increase in synchrotron radiation emission as a function of the beam energy scattering and absorption in related frequency [9,10]. Synchrotron radiation emission as a function of the beam energy absorption and induced produced heat in nanoparticles has been considered as a side effect in plasmonic applications for a long time [11-15]. Recently, scientists find that the thermoplasmonic characteristic can be used for various optothermal applications in cancer, nanoflows and photonic [16-22]. In optothermal human cancer cells, tissues and tumors treatment, the descendent laser light stimulate resonance of surface plasmon of metallic nanoparticles and as a result of this process, the absorbed energy of descendent light converse to heat in nanoparticles [23-25]. The produced heat devastates tumor tissue adjacent to nanoparticles without any hurt to sound tissues [26,27]. Regarding the simplicity of ligands connection to dysprosium nanoparticles for targeting cancer cells, these nanoparticles are more appropriate to use in optothermal human cancer cells, tissues and tumors treatment [28-36]. In the current paper, thermoplasmonic characteristics of spherical, core-shell and rod dysprosium nanoparticles are investigated.

Author affiliations:

[1]Faculty of Chemistry, California South University, 14731 Comet St. Irvine, CA 92604, USA
[2]American International Standards Institute, Irvine, CA 3800, USA

✉To whom correspondence to be addressed:

E-mail: Scholar.Researcher.Scientist@gmail.com; Alireza.Heidari@calsu.us; Central@aisi-usa.org

Available online at: http://ajmc.asianpubs.org

Heat generation in synchrotron radiation emission as a function of the beam energy-dysprosium nanoparticles interaction: When dysprosium nanoparticles are subjected to descendent light, a part of light scattered (emission process) and the other part absorbed (non-emission process). The amount of energy dissipation in non-emission process mainly depends on material and volume of nanoparticles and it can be identified by absorption cross section. At the other hand, emission process which its characteristics depend on volume, shape and surface characteristics of nanoparticles explains by scattering cross section. Sum of absorption and scattering processes which lead to light dissipation is called extinction cross section [37-40].

Dysprosium nanoparticles absorb energy of descendent light and generate some heat in the particle. The generated heat transferred to the surrounding environment and leads to increase in temperature of adjacent points to nanoparticles. Heat variations can be obtained by heat transfer equation [41,42].

Simulation: To calculate the generated heat in dysprosium nanoparticles, COMSOL software, which works by Finite element method (FEM) was used. All simulations were made in 3D. Firstly, absorption and scattering cross section areas were calculated by optical module of software. Then, using heat module, temperature variations of nanoparticles and its surrounding environment were calculated by data from optical module. In all cases, dysprosium nanoparticles are presented in water environment with dispersion coefficient of 1.84 and are subjected to flat wave emission with linear polarization. Intensity of descendent light is 1 mW/μm^2. Dielectric constant of dysprosium is dependent on particle size.

Firstly, calculations were made for dysprosium nanospheres with radius of 5, 10, 15, 20, 25, 30, 35, 40, 45 and 50 nm. The results show that by increase in nanoparticles size, extinction cross section area increases and maximum wavelength slightly shifts toward longer wavelengths. The maximum increase in temperature of nanospheres in surface plasmon frequency is shown in Fig. 1.

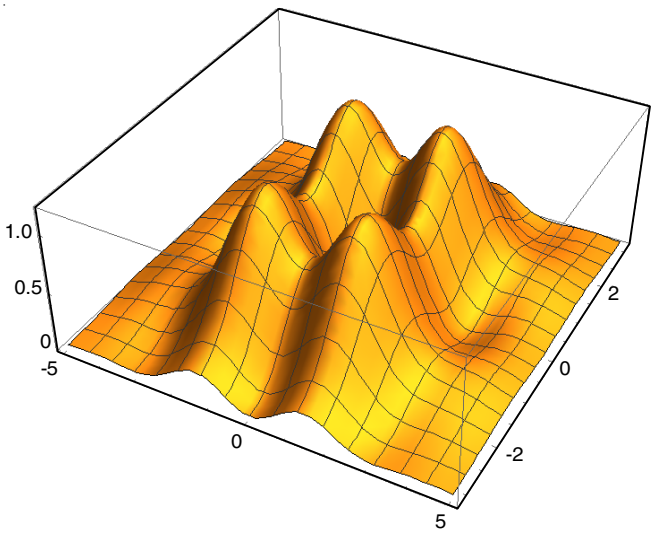

Fig. 1. Maximum increase in temperature for dysprosium nanospheres

According to the graph, it can be seen that the generated heat is increased by increase in nanoparticles size. For 100 nm nanoparticles (sphere with 50 nm radius), the maximum increase in temperature is 83 K. When nanoparticles size reaches to 150 nm, increase in temperature is increased in spite of increase in extinction coefficient. In order to find the reason of this fact, ratio of absorption to extinction for various nanospheres in plasmon frequency is shown in Fig. 2.

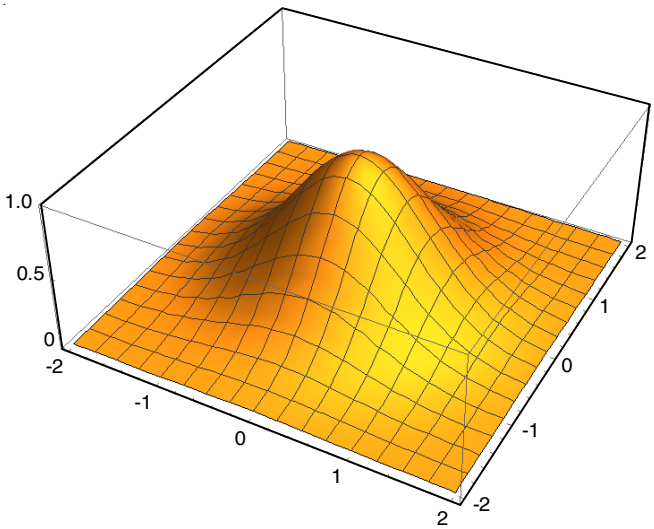

Fig. 2. Variations of absorption to extinction ratio and scattering to extinction ratio for dysprosium nanospheres with various radii

Fig. 2 shows that increasing the size of nanospheres leads to decrease in ratio of light absorption to total energy of descendent light so that for 150 nm nanosphere, scattering is larger than absorption. It seems that although increase in nanoparticles size leads to more dissipation of descendent light, the dissipation is in the form of scattering and hence, it cannot be effective on heat generation.

Heat distribution (Fig. 3) shows that temperature is uniformly distributed throughout the nanoparticles, which are due to high thermal conductivity of dysprosium.

In this section, core-shell structure of dysprosium and silica is chosen. The core of a nanosphere with 45 nm radius and silica layer thickness of 5, 10, 15, 20, 25, 30, 35, 40, 45 and 50 nm are considered. The results show that increase in silica thickness leads to increase in extinction coefficient and shift in plasmon wavelength of nanoparticles, to some extent.

According to Fig. 4, silica shell causes to considerable increase in temperature of dysprosium nanoparticles but by more increase in silica thickness, its effects are decreased. Heat distribution (Fig. 5) shows that temperature is uniformly distributed throughout metallic core as well as silica shell. However, silica temperature is considerably lower than core temperature due to its lower thermal conductivity. In fact, silica layer prohibits heat transfer from metal to the surrounding aqueous environment due to low thermal conductivity and hence, temperature of nanoparticles has more increase in temperature. Increasing the thickness of silica shell leads to increase in its thermal conductivity and hence, leads to attenuate in increase in nanoparticles temperature.

The graphs (Fig. 6) show that the variation of nanorod dimension ratio leads to considerable shift in plasmon wavelength. This fact allows regulating the plasmon frequency

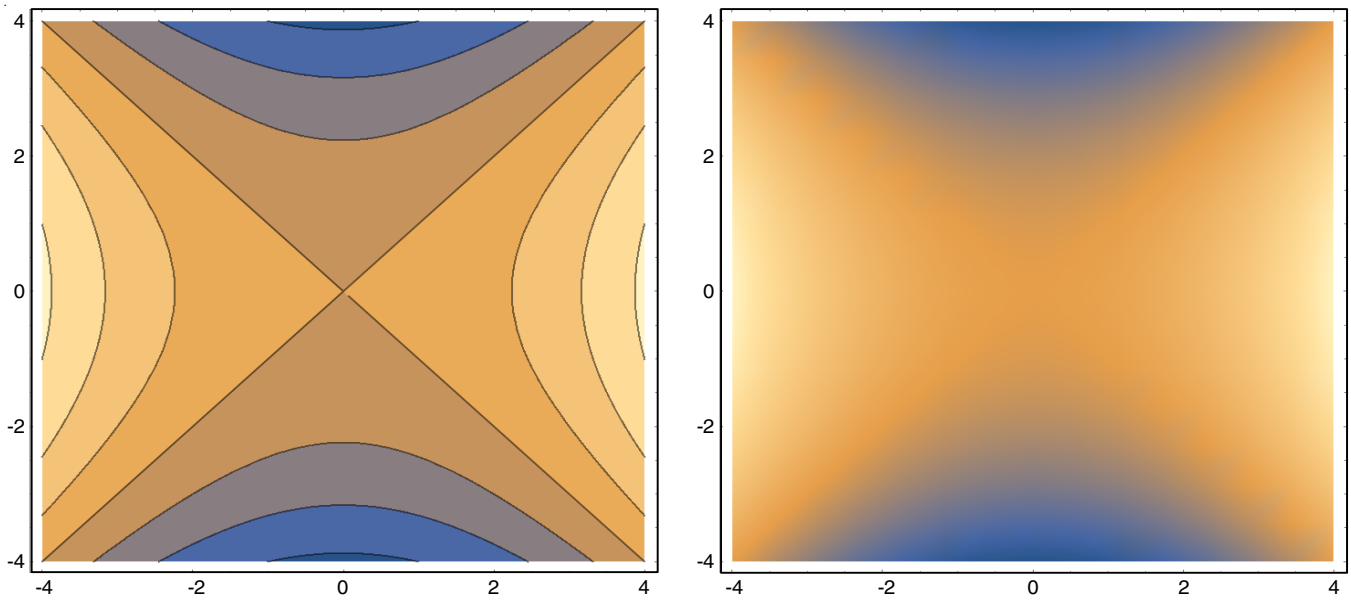

Fig. 3. Maximum increase in temperature for spherical nanoparticles with radius of 45 nm at plasmon wavelength of 685 nm

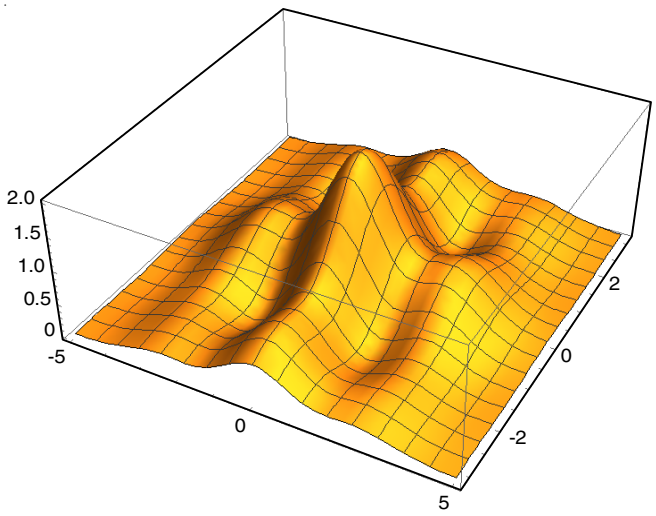

Fig. 4. Maximum increase in temperature for core-shell dysprosium nanospheres with various thicknesses of silica shell

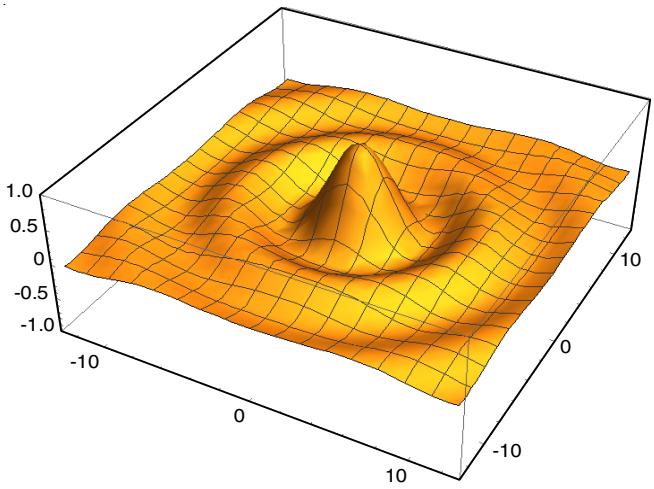

Fig. 5. Maximum increase in temperature for core-shell nanoparticles with radius of 45 nm and silica thickness of 10 nm at plasmon wavelength of 701 nm

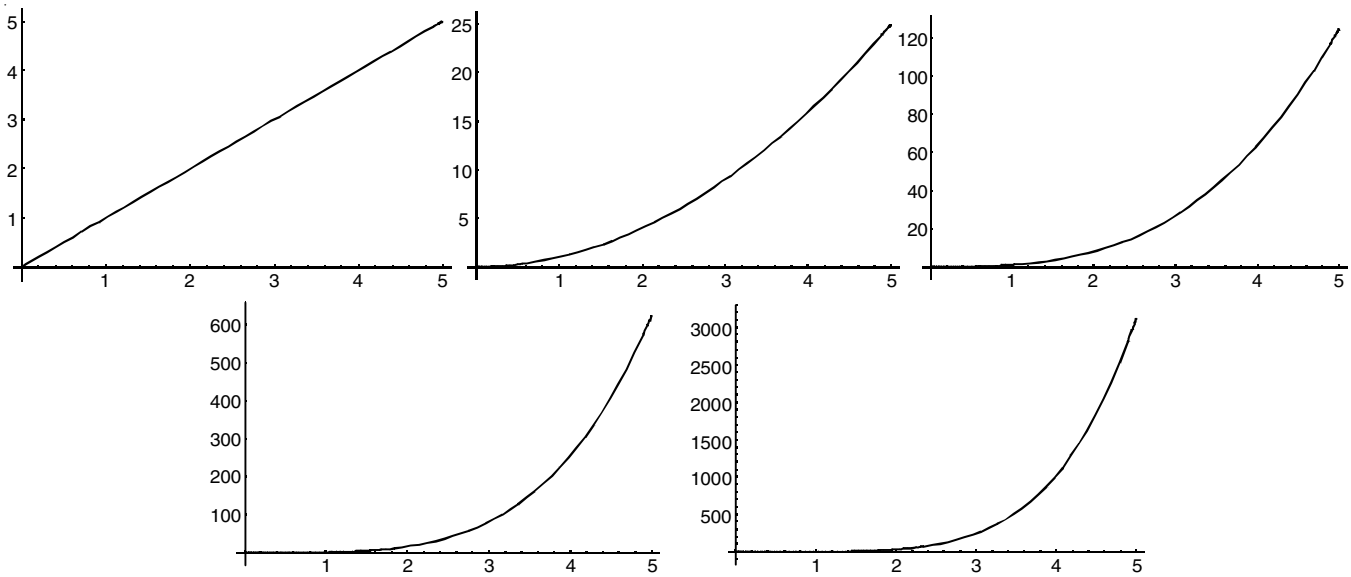

Fig. 6. Extinction cross section area for dysprosium nanorods with effective radius of 45 nm and various dimension ratios

to place in near IR zone. Light absorption by body tissues is lower in this zone of spectrum and hence, nanorods are more appropriate for optothermal human cancer cells, tissues and tumors treatment methods.

Variations of temperature in dysprosium nanorods with two effective radius and various dimension ratios are shown in Fig. 7. By increase in length (a) to radius (b) of nanorod, temperature is increased.

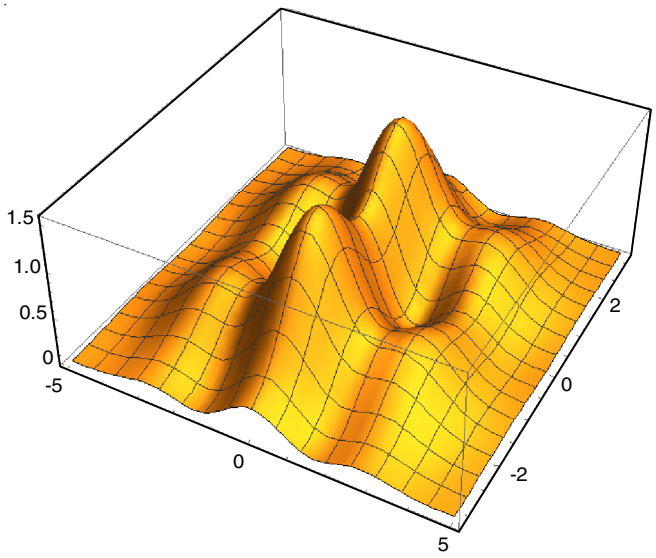

Fig. 7. Maximum increase in temperature for nanorods with effective radius of 20 and 45 nm and various dimension ratios

Conclusion

The calculations showed that in dysprosium nanoparticles, light absorption in plasmon frequency causes to increase in temperature of the surrounding environment of nanoparticles. In addition, it showed that adding a thin silica layer around the dysprosium nanospheres increases their temperatures. Calculations of nanorods showed that due to ability for shifting surface plasmon frequency toward longer wavelength as well as more increase in temperature, this nanostructure is more appropriate for medical applications such as optothermal human cancer cells, tissues and tumors treatments.

ACKNOWLEDGEMENTS

Authors are financially supported by an American International Standards Institute (AISI) Future Fellowship Grant FT12010 093734710. We acknowledge Ms. Isabelle Villena for instrumental support and Dr. Michael N. Cocchi for constructing graphical abstract figures. We gratefully acknowledge Prof. Dr. Christopher Brown for proof reading the manuscript. Synchrotron beam time was awarded by the National Synchrotron Light Source (NSLS-II) under the merit-based proposal scheme.

REFERENCES

1. P. Yu, J. Wu, S. Liu, J. Xiong, C. Jagadish and Z.M. Wang, Design and Fabrication of Silicon Nanowires Towards Efficient Solar Cells, *Nano Today*, **11**, 704 (2016); https://doi.org/10.1016/j.nantod.2016.10.001.
2. S. Sandhu and S. Fan, Current–Voltage Enhancement of a Single Coaxial Nanowire Solar Cell, *ACS Photonics*, **2**, 1698 (2015); https://doi.org/10.1021/acsphotonics.5b00236.
3. D. van Dam, N.J.J. Van Hoof, Y. Cui, P.J. van Veldhoven, E.P.A.M. Bakkers, J. Gómez Rivas and J.E.M. Haverkort, High-Efficiency Nanowire Solar Cells with Omnidirectionally Enhanced Absorption Due to Self-Aligned Indium-Tin-Oxide Mie Scatterers, *ACS Nano*, **10**, 11414 (2016); https://doi.org/10.1021/acsnano.6b06874.
4. S. Luo, W.B. Yu, Y. He and G. Ouyang, Size-Dependent Optical Absorption Modulation of Si/Ge And Ge/Si Core/Shell Nanowires with Different Cross-Sectional Geometries, *Nanotechnology*, **26**, 085702 (2015); https://doi.org/10.1088/0957-4484/26/8/085702.
5. P. Yu, Y. Yao, J. Wu, X. Niu, A.L. Rogach and Z. Wang, Effects of Plasmonic Metal Core -Dielectric Shell Nanoparticles on the Broadband Light Absorption Enhancement in Thin Film Solar Cells, *Sci. Rep.*, **7**, 7696 (2017); https://doi.org/10.1038/s41598-017-08077-9.
6. A.M. Gouda, N.K. Allam and M.A. Swillam, Efficient Fabrication Methodology of Wide Angle Black Silicon for Energy Harvesting Applications, *RSC Adv.*, **7**, 26974 (2017); https://doi.org/10.1039/C7RA03568C.
7. H.M. Branz, V.E. Yost, S. Ward, K.M. Jones, B. To and P. Stradins, Nanostructured Black Silicon and the Optical Reflectance of Graded-Density Surfaces, *Appl. Phys. Lett.*, **94**, 231121 (2009); https://doi.org/10.1063/1.3152244.
8. B. Fazio, P. Artoni, M. Antonía Iatí, C. D'Andrea, M.J. Lo Faro, S. Del Sorbo, S. Pirotta, P. Giuseppe Gucciardi, P. Musumeci, C. Salvatore Vasi, R. Saija, M. Galli, F. Priolo and A. Irrera, Strongly Enhanced Light Trapping in a Two-dimensional Silicon Nanowire Random Fractal Array, *Light Sci. Appl.*, **5**, e16062 (2016); https://doi.org/10.1038/lsa.2016.62.
9. M.-D. Ko, T. Rim, K. Kim, M. Meyyappan and C.-K. Baek, High Efficiency Silicon Solar Cell Based on Asymmetric Nanowire, *Sci. Rep.*, **5**, 11646 (2015); https://doi.org/10.1038/srep11646.
10. J. Oh, H.C. Yuan and H.M. Branz, An 18.2%-Efficient Black-silicon Solar Cell Achieved Through Control of Carrier Recombination in Nanostructures, *Nat. Nanotechnol.*, **7**, 743 (2012); https://doi.org/10.1038/nnano.2012.166.
11. H. Lin, F. Xiu, M. Fang, S. Yip, H.Y. Cheung, F. Wang, N. Han, K.S. Chan, C.Y. Wong and J.C. Ho, Rational Design of Inverted Nanopencil Arrays for Cost-Effective, Broadband and Omnidirectional Light Harvesting, *ACS Nano*, **8**, 3752 (2014); https://doi.org/10.1021/nn500418x.
12. E. Garnett and P. Yang, Light Trapping in Silicon Nanowire Solar Cells, *Nano Lett.*, **10**, 1082 (2010); https://doi.org/10.1021/nl100161z.
13. S. Misra, L. Yu, M. Foldyna and I.R. i Cabarrocas, High Efficiency and Stable Hydrogenated Amorphous Silicon Radial Junction Solar Cells Built on VLS-Grown Silicon Nanowires, *Sol. Energy Mater. Sol. Cells*, **118**, 90 (2013); https://doi.org/10.1016/j.solmat.2013.07.036.
14. M.D. Kelzenberg, S.W. Boettcher, J.A. Petykiewicz, D.B. Turner-Evans, M.C. Putnam, E.L. Warren, J.M. Spurgeon, R.M. Briggs, N.S. Lewis and H.A. Atwater, Enhanced Absorption and Carrier Collection in Si Wire Arrays for Photovoltaic Applications, *Nat. Mater.*, **9**, 239 (2010); https://doi.org/10.1038/nmat2635.
15. B. Tian, X. Zheng, T.J. Kempa, Y. Fang, N. Yu, G. Yu, J. Huang and C.M. Lieber, Coaxial Silicon Nanowires as Solar Cells and Nanoelectronic Power Sources, *Nature*, **449**, 885 (2007); https://doi.org/10.1038/nature06181.
16. S.A. Razek, M.A. Swillam and N.K. Allam, Vertically Aligned Crystalline Silicon Nanowires with Controlled Diameters for Energy Conversion Applications: Experimental and Theoretical Insights, *J. Appl. Phys.*, **115**, 194305 (2014); https://doi.org/10.1063/1.4876477.
17. N. Dhindsa, J. Walia and S.S. Saini, A Platform for Colorful Solar Cells with Enhanced Absorption, *Nanotechnology*, **27**, 495203 (2016); https://doi.org/10.1088/0957-4484/27/49/495203.
18. N. Dhindsa, J. Walia, M. Pathirane, I. Khodadad, W.S. Wong and S.S. Saini, Adjustable Optical Response of Amorphous Silicon Nanowires Integrated with Thin Films, *Nanotechnology*, **27**, 145703 (2016); https://doi.org/10.1088/0957-4484/27/14/145703.

19. J. Zhu, Z. Yu, G.F. Burkhard, C.-M. Hsu, S.T. Connor, Y. Xu, Q. Wang, M. McGehee, S. Fan and Y. Cui, Optical Absorption Enhancement in Amorphous Silicon Nanowire and Nanocone Arrays, *Nano Lett.*, **9**, 279 (2009); https://doi.org/10.1021/nl802886y.
20. D. Klinger, E. £usakowska and D. Zymierska, Nano-Structure Formed by Nanosecond Laser Annealing on Amorphous Si Surface, *Mater. Sci. Semicond. Process.*, **9**, 323 (2006); https://doi.org/10.1016/j.mssp.2006.01.027.
21. P. Kumar, M.G. Krishna and A. Bhattacharya, Excimer Laser Induced Nanostructuring of Silicon Surfaces, *J. Nanosci. Nanotechnol.*, **9**, 3224 (2009); https://doi.org/10.1166/jnn.2009.207.
22. P. Kumar, Surface Modulation of Silicon Surface by Excimer Laser at Laser Fluence below Ablation Threshold, *Appl. Phys., A Mater. Sci. Process.*, **99**, 245 (2010); https://doi.org/10.1007/s00339-009-5510-x.
23. A.A.D.T. Adikaari and S.R.P. Silva, Thickness Dependence of Properties of Excimer Laser Crystallized Nano-Polycrystalline Silicon, *J. Appl. Phys.*, **97**, 114305 (2005); https://doi.org/10.1063/1.1898444.
24. A.A.D.T. Adikaari, D.M.N.M. Dissanayake, R.A. Hatton and S.R.P. Silva, Efficient Laser Textured Nanocrystalline Silicon-Polymer Bilayer Solar Cells, *Appl. Phys. Lett.*, **90**, 203514 (2007); https://doi.org/10.1063/1.2739365.
25. A.A.D.T. Adikaari and S.R.P. Silva, Excimer Laser Crystallization and Nanostructuring of Amorphous Silicon for Photovoltaic Applications, *Nano*, **3**, 117 (2008); https://doi.org/10.1142/S1793292008000915.
26. Y.F. Tang, S.R.P. Silva, B.O. Boskovic, J.M. Shannon and M.J. Rose, Electron Field Emission from Excimer Laser Crystallized Amorphous Silicon, *Appl. Phys. Lett.*, **80**, 4154 (2002); https://doi.org/10.1063/1.1482141.
27. S. Jin, S. Hong, M. Mativenga, B. Kim, H.H. Shin, J.K. Park, T.W. Kim and J. Jang, Low Temperature Polycrystalline Silicon with Single Orientation on Glass by Blue Laser Annealing, *Thin Solid Films*, **616**, 838 (2016); https://doi.org/10.1016/j.tsf.2016.10.026.
28. Y. Jiang, X. Gong, R. Qin, H. Liu, C. Xia and H. Ma, Efficiency Enhancement Mechanism for Poly(3,4-ethylenedioxythiophene): Poly-(styrenesulfonate)/Silicon Nanowires Hybrid Solar Cells using Alkali Treatment, *Nanoscale Res. Lett.*, **11**, 267 (2016); https://doi.org/10.1186/s11671-016-1450-5.
29. T.T.T. N'Guyen, H.T.T. Duong, J. Basuki, V. Montembault, S. Pascual, C. Guibert, J. Fresnais, C. Boyer, M.R. Whittaker, T.P. Davis and L. Fontaine, Functional Iron Oxide Magnetic Nanoparticles with Hyperthermia-Induced Drug Release Ability by Using a Combination of Orthogonal Click Reactions, *Angew. Chem. Int. Ed.*, **52**, 14152 (2013); https://doi.org/10.1002/anie.201306724.
30. Z. Xu, Y. Zhao, X. Wang and T. Lin, A Thermally Healable Polyhedral Oligomeric Silsesquioxane (POSS) Nanocomposite Based on Diels–Alder Chemistry, *Chem. Commun.*, **49**, 6755 (2013); https://doi.org/10.1039/c3cc43432j.
31. M. Torres-Lugo and C. Rinaldi, Thermal Potentiation of Chemotherapy by Magnetic nanoparticles, *Nanomedicine*, **8**, 1689 (2013); https://doi.org/10.2217/nnm.13.146.
32. S. Schäfer and G. Kickelbick, Self-healing Polymer Nanocomposites Based on Diels-alder Reactions with Silica Nanoparticles: The Role of the Polymer Matrix, *Polymer*, **69**, 357 (2015); https://doi.org/10.1016/j.polymer.2015.03.017.
33. B.A. Larsen, K.M. Hurst, W.R. Ashurst, N.J. Serkova and C.R. Stoldt, Mono and Dialkoxysilane Surface Modification of Superparamagnetic Iron Oxide Nanoparticles for Application as Magnetic Resonance Imaging Contrast Agents, *J. Mater. Res.*, **27**, 1846 (2012); https://doi.org/10.1557/jmr.2012.160.
34. K. Davis, B. Qi, M. Witmer, C.L. Kitchens, B.A. Powell and O.T. Mefford, Quantitative Measurement of Ligand Exchange on Iron Oxides *via* Radiolabeled Oleic Acid, *Langmuir*, **30**, 10918 (2014); https://doi.org/10.1021/la502204g.
35. R. Sauer, P. Froimowicz, K. Scholler, J.M. Cramer, S. Ritz, V. Mailander and K. Landfester, Design, Synthesis and Miniemulsion Polymerization of New Phosphonate Surfmers and Application Studies of the Resulting Nanoparticles as Model Systems for Biomimetic Mineralization and Cellular Uptake, *Chem. Eur. J.*, **18**, 5201 (2012); https://doi.org/10.1002/chem.201103256.
36. V. Patsula, L. Kosinova, M. Lovric, L. Ferhatovic Hamzic, M. Rabyk, R. Konefal, A. Paruzel, M. Slouf, V. Herynek, S. Gajovic and D. Horak, Superparamagnetic Fe_3O_4 Nanoparticles: Synthesis by Thermal Decomposition of Iron(III) Glucuronate and Application in Magnetic Resonance Imaging, *ACS Appl. Mater. Interfaces*, **8**, 7238 (2016); https://doi.org/10.1021/acsami.5b12720.
37. N. Pothayee, S. Balasubramaniam, R.M. Davis, J.S. Riffle, M.R.J. Carroll, R.C. Woodward and T.G. St. Pierre, Synthesis of 'Ready-To-Adsorb' Polymeric Nanoshells for Magnetic Iron Oxide Nanoparticles *via* Atom Transfer Radical Polymerization, *Polymer*, **52**, 1356 (2011); https://doi.org/10.1016/j.polymer.2011.01.047.
38. L. Breucker, K. Landfester and A. Taden, Phosphonic Acid-Functionalized Polyurethane Dispersions with Improved Adhesion Properties, *ACS Appl. Mater. Interfaces*, **7**, 24641 (2015); https://doi.org/10.1021/acsami.5b06903.
39. R.C. Longo, K. Cho, W.G. Schmidt, Y.J. Chabal and P. Thissen, Monolayer Doping *via* Phosphonic Acid Grafting on Silicon: Microscopic Insight from Infrared Spectroscopy and Density Functional Theory Calculations, *Adv. Funct. Mater.*, **23**, 3471 (2013); https://doi.org/10.1002/adfm.201202808.
40. Y. Lalatonne, C. Paris, J.M. Serfaty, P. Weinmann, M. Lecouvey and L. Motte, Bis-Phosphonates–Ultra Small Superparamagnetic Iron Oxide Nanoparticles: A Platform Towards Diagnosis and Therapy, *Chem. Commun.*, 2553 (2008); https://doi.org/10.1039/b801911h.
41. J. Eizenkop, I. Avrutsky, D.G. Georgiev and V. Chaudchary, Single-Pulse Excimer Laser Nanostructuring of Silicon: A Heat Transfer Problem and Surface Morphology, *J. Appl. Phys.*, **103**, 094311 (2008); https://doi.org/10.1063/1.2910196.
42. J. Eizenkop, I. Avrutsky, G. Auner, D.G. Georgiev and V. Chaudhary, Single Pulse Excimer Laser Nanostructuring of Thin Silicon Films: Nanosharp Cones Formation and a Heat Transfer Problem, *J. Appl. Phys.*, **101**, 094301 (2007); https://doi.org/10.1063/1.2720185.